Check for updates

Received: 22 December 2020 | Revised: 5 March 2021 | Accepted: 26 March 2021

DOI: 10.1002/aoc.6261

FULL PAPER

Applied Organometallic Chemistry WILEY

Nickel(II) complexes with N,O-donor thiopseudourea ligands: Syntheses, structures, and catalytic applications in Kumada–Corriu cross-coupling reactions

Kinche Shakunthala | **Ankit Kumar Srivastava** | **G. Narendra Babu** | **Srinivas Keesara** | **Samudranil Pal**

School of Chemistry, University of Hyderabad, Hyderabad, 500046, India

Correspondence
Samudranil Pal, School of Chemistry, University of Hyderabad, Hyderabad 500046, India.
Email: spal@uohyd.ac.in

Funding information
University Grants Commission, Grant/Award Numbers: 187/(CSIR-UGC NET June 2017), F.540/2/CAS-111/2016(SAP-I), F.4-2/2006(BSR)/13-1125/2013(BSR), F.25-1/2014-15(BSR)/5-129/2007(BSR); Department of Science and Technology (DST), New Delhi, Grant/Award Number: SR/FST/CST-030/2014(C); Ministry of Education, Government of India, Grant/Award Number: F11/9/2019-U3(A); Council of Scientific and Industrial Research, India, Grant/Award Number: 09/414(1025)/2012-EMR-I

Synthesis, characterization, and physical properties of benzyl-*N*′-(4-R-benzoyl)-*N*-(2,6-diisopropylphenyl)carbamimidothioates, HL^1 (R = H) and HL^2 (R = Cl), and their nickel(II) complexes having the general molecular formula $[Ni(L^{1/2})_2]$ (**1** and **2**) have been reported. Elemental analysis, magnetic susceptibility, solution electrical conductivity, and various spectroscopic (IR, UV–Vis, and ^1H NMR) measurements were used to characterize HL^1, HL^2, and the two complexes (**1** and **2**). The molecular structures of all four compounds were determined by single-crystal X-ray crystallographic studies. The structures of HL^1 and HL^2 showed the imino-ketone form of both compounds. In each of **1** and **2**, the six-membered chelate ring forming iminolate-O and azomethine-N donor two $(L^{1/2})^-$ ligands form a square-planar *trans*-N_2O_2 coordination environment around the metal center. The spectroscopic characteristics of HL^1, HL^2, **1**, and **2** are consistent with their molecular structures. Both complexes were successfully employed as efficient catalysts in Kumada–Corriu C—C cross-coupling reactions of aryl bromides with phenylmagnesium bromide. The reactions provided biaryl products in good to excellent yields with a good substrate scope.

KEYWORDS

crystal structure, Kumada–Corriu reaction, nickel(II), NO-donor, thiopseudourea

1 | INTRODUCTION

Transition metal catalyzed cross-coupling reaction leading to the formation of C—C bond is a powerful and widely used tool for the synthesis of natural products and a variety of complex and structurally intricate organic compounds with potential for use as agrochemicals, pharmaceuticals, and functional materials.[1,2] The biaryl frameworks are widespread and play important roles in deciding the properties and activities of these types of compounds. Hence, in recent years, the syntheses of biaryls via C—C cross-coupling reactions have attracted particular attention.[2] Generally, complexes of palladium, the 4d-block transition metal in Group 10, are found to be the most efficient catalysts for the various cross-coupling reactions. However, due to the high cost of palladium, there is a continuous quest for less expensive and environment friendly alternative to these palladium catalysts. As a result, complexes of nickel, the lightest and inexpensive member of Group 10, have attracted immense attention as catalysts for cross-coupling reaction.[3–6] The first nickel catalyzed C—C cross-coupling reaction using alkyl or aryl halides, and Grignard reagents were reported independently by

https://doi.org/10.1002/aoc.6261

© 2021 John Wiley & Sons, Ltd.

Tamao et al.[3] and Corriu and Masse[4] in 1972. Since then, a large number of nickel complexes with a variety of ligands such as Schiff bases, monophosphines/diphosphines/triphosphines, diamines, β-diketonates, *N*-heterocyclic carbenes, and various pincer ligands have been employed for this cross-coupling reaction.[5,6] Thiourea, isothiourea, and thiopseudourea derivatives are of considerable interest for their complexation behaviors and applications as catalysts as well as for their biological and biochemical properties leading to various therapeutic and diagnostic applications.[7–9] In this work, we have examined the coordination behavior of two thiopseudoureas benzyl-*N*′-(4-R-benzoyl)-*N*-(2,6-diisopropylphenyl)carbamimidothioates (HL^n, where $n = 1$ and 2 for R = H and Cl, respectively) toward nickel(II) (Scheme 1) and the catalytic activities of the resulting complexes in Kumada–Corriu cross-coupling reaction. The deprotonated thiopseudourea system $(L^n)^-$ can act as a bidentate six-membered chelate ring forming ligand in two ways: via iminolate-O and thioether-S coordination or via iminolate-O and azomethine-N coordination. Considering the moderately soft character of nickel(II) and the sterically crowded environment of the azomethine-N, it was anticipated that $(L^n)^-$ may prefer the O,S-coordination mode rather than the O,N-coordination mode. In a somewhat similar situation, it has been found that *N*,*N*-dialkyl/diaryl-*N*′-(aroyl) thioureates $(L)^-$ provide square-planar nickel(II) complexes $[NiL_2]$, where $(L)^-$ coordinates the metal center through the O-atom and the less crowded S-atom instead of the N-atom containing two alkyl groups.[7] It may be noted that like the present ligand system, each of these thioureates $(L)^-$ also forms six-membered chelate ring at the metal center in either O,S- or O,N-coordination mode. Interestingly, the present thiopseudourea ligand system $(L^n)^-$ behaves in the opposite way and acts as O,N-donor in the two complexes having the general formula $[Ni(L^n)_2]$ (**1** and **2** where $n = 1$ and 2, respectively) (Scheme 1). Herein, we report the syntheses, characterization, and X-ray structures of $HL^{1/2}$ and their complexes $[Ni(L^{1/2})_2]$ (**1** and **2**). Application of both complexes as effective catalysts in Kumada–Corriu C—C cross-coupling reactions of aryl bromides with phenylmagnesium bromide has been demonstrated.

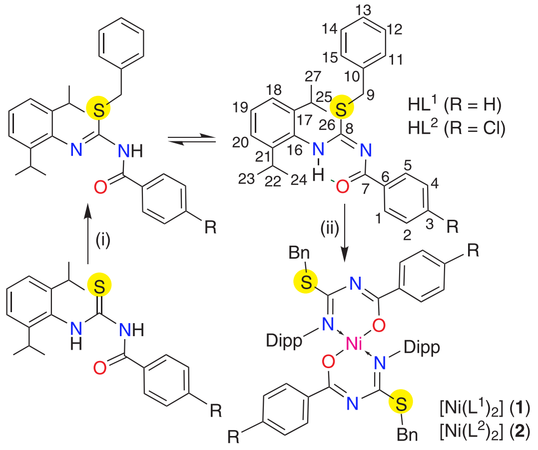

SCHEME 1 Syntheses of $HL^{1/2}$ and $[Ni(L^{1/2})_2]$ (**1** and **2**): (i) $PhCH_2Br$ and NaH in tetrahydrofuran at 0°C for 3 h. (ii) $Ni(OAc)_2{\cdot}4H_2O$ in MeOH–$CHCl_3$ (1:1) at 50°C for 24 h

2 | EXPERIMENTAL

2.1 | Materials

Aryl halides and phenylmagnesium bromide for the cross-coupling reactions were procured from Sigma-Aldrich and were used as received. The *N*-(4-R-benzoyl)-*N*′-(2,6-diisopropylphenyl)thioureas (R = H and Cl) were prepared in about 90% yields from 4-R-benzoyl chlorides (R = H and Cl), NH_4SCN, and 2,6-diisopropylaniline by following a reported procedure.[9] All other chemicals used in this work were of reagent grade available commercially and were used without further purification. All solvents used were purified by standard methods.[10]

2.2 | Physical measurements

Elemental (CHN) analyses were performed on a Thermo Finnigan Flash EA1112 series elemental analyzer. A Sherwood scientific balance was used for the magnetic susceptibility measurements. A Digisun DI-909 conductivity meter was used to measure the electrical conductivities in solution. The infrared spectra were recorded with a Bruker TENSOR II FT-IR spectrophotometer. A Shimadzu UV-3600 UV–Vis–NIR spectrophotometer was used to collect the electronic spectra. The ^1H NMR spectra were recorded using a Bruker NMR spectrometer.

2.3 | Synthetic procedures

2.3.1 | Benzyl-*N*′-(4-R-benzoyl)-*N*-(2,6-diisopropylphenyl) carbamimidothioates (HL^n)

Benzyl bromide (0.36 ml, 518 mg, 3 mmol) was added dropwise to a solution of *N*-(4-R-benzoyl)-*N*′-(2,6-diisopropylphenyl)thiourea (R = H or Cl) (3 mmol) and NaH (60% in mineral oil, 200 mg, 5 mmol) in tetrahydrofuran (50 ml) and stirred at 0°C for 3 h. The reaction mixture was then neutralized with aqueous NH_4Cl, and the organic layer was extracted with ethyl acetate (2×50 ml), dried over $MgSO_4$, filtered, and finally, the filtrate was evaporated to dryness in vacuum to obtain the crude product. It was then purified by column chromatography on silica gel using ethyl acetate–*n*-hexane mixture (1:9) as the eluent. The solution obtained was evaporated to dryness and the product was isolated as white solid.

HL^1: Yield 1.1 g (85%). Anal. Calcd for $C_{27}H_{30}N_2OS$ (430.59) (%): C, 75.31. H, 7.02. N, 6.51. Found (%): C, 75.26. H, 7.12. N, 6.63. Selected IR bands (cm^{-1}): 3165 (NH), 1653 (C=O), 1598 (C=N). ^1H NMR ($CDCl_3$. 500 MHz, δ [J], ppm [Hz]): 12.45 (s, 1H, NH), 8.38 (8) (d, 2H, $H^{1,5}$), 7.55 (8) (t, 1H, H^3), 7.48 (8) (dd → t, 2H, $H^{2,4}$), 7.39–7.35 and 7.29–7.23 (both m, 3H, 3H, $H^{11-15,19}$), 7.21 (8) (d, 2H, $H^{18,20}$), 4.55 (s, 2H, $H^{9a,b}$), 3.14 (7) (sep, 2H, $H^{22,25}$), 1.25 (7) (d, 6H, Me-protons of dipp), 1.18 (7) (d, 6H, Me-protons of dipp).

HL^2: Yield 1.2 g (86%). Anal. Calcd for $C_{27}H_{29}N_2ClOS$ (465.03) (%): C, 69.73. H, 6.29. N, 6.02. Found (%): C, 69.85. H, 6.35. N, 6.12. Selected IR bands (cm^{-1}): 3199 (NH), 1686 (C=O), 1598 (C=N). ^1H NMR ($CDCl_3$. 500 MHz, δ [J], ppm [Hz]): 12.40 (s, 1H, NH), 8.29 (9) (d, 2H, $H^{1,5}$), 7.44 (9) (d, 2H, $H^{2,4}$), 7.40–7.33 and 7.30–7.24 (both m, 3H, 3H, $H^{11-15,19}$), 7.22 (8) (d, 2H, $H^{18,20}$), 4.52 (s, 2H, $H^{9a,b}$), 3.13 (7) (sep, 2H, $H^{22,25}$), 1.26 (7) (d, 6H, Me-protons of dipp), 1.18 (7) (d, 6H, Me-protons of dipp).

2.3.2 | $[Ni(L^1/L^2)_2]$ (1 and 2)

A methanol solution (30 ml) of $Ni(OAc)_2 \cdot 4H_2O$ (249 mg, 1 mmol) was added to a chloroform solution (30 ml) of HL^n (2 mmol), and the mixture was stirred at 50°C for 24 h. The reaction mixture was then evaporated under reduced pressure, and the solid obtained was washed with water and then dried in a vacuum desiccator. The dry solid was dissolved in chloroform (15 ml). To this chloroform solution methanol (15 ml) was added with stirring. The light brown solid separated was collected by filtration and dried in air.

$[Ni(L^1)_2]$ (**1**): Yield 630 mg (69%). Anal. Calcd for $C_{54}H_{58}N_4O_2S_2Ni$ (917.87) (%): C, 70.66. H, 6.37. N, 6.10. Found (%): C, 70.65. H, 6.52. N, 6.15. Selected IR band (cm^{-1}): 1589 (C=N). UV–Vis ($CHCl_3$; λ_{max} (nm) (ε [M^{-1} cm^{-1}])): 600^{sh} (47), 502 (131), 395^{sh} (2.7×10^3), 355^{sh} (1.3×10^4), 330^{sh} (1.9×10^4), 303 (2.8×10^4), 253 (2.1×10^4). ^1H NMR ($CDCl_3$; 500 MHz, δ [J], ppm [Hz]): 7.42 (9) (t, 1H, H^{19}), 7.28 (8) (t, 1H, H^3), 7.23–7.16 (m, 7H, $H^{1,2,4,5,11,13,15}$), 7.04 (9) (dd → t, 2H, $H^{12,14}$), 6.74 (9) (d, 2H, $H^{18,20}$), 4.35 (s, 2H, $H^{9a,b}$), 4.15 (9) (sep, 2H, $H^{22,25}$), 1.42 (9) (d, 6H, Me-protons of dipp), 1.33 (9) (d, 6H, Me-protons of dipp).

$[Ni(L^2)_2]$ (**2**): Yield 690 mg (70%). Anal. Calcd for $C_{54}H_{56}N_4O_2Cl_2S_2Ni$ (986.76) (%): C, 65.73. H, 5.72. N, 5.68. Found (%): C, 65.46. H, 5.85. N, 5.58. Selected IR band (cm^{-1}): 1579 (C=N). UV–Vis ($CHCl_3$; λ_{max} (nm) (ε [M^{-1} cm^{-1}])): 600^{sh} (56), 502 (152), 400^{sh} (2.3×10^3), 357^{sh} (1.2×10^4), 330^{sh} (1.8×10^4), 304 (2.3×10^4), 252 (1.7×10^4). ^1H NMR ($CDCl_3$; 500 MHz, δ [J], ppm [Hz]): 7.42 (8) (t, 1H, H^{19}), 7.24–7.16 (m, 7H, $H^{1,5,11-15}$), 6.99 (9) (d, 2H, $H^{2,4}$), 6.61 (8) (d, 2H, $H^{18,20}$), 4.30 (s, 2H, $H^{9a,b}$), 4.11 (7) (sep, 2H, $H^{22,25}$), 1.40 (7) (d, 6H, Me-protons of dipp), 1.33 (7) (d, 6H, Me-protons of dipp).

2.4 | X-ray crystallography

X-ray quality single crystals of HL^1 and HL^2 were obtained by slow evaporation of their solutions in ethyl acetate–*n*-hexane (1:10) mixture, whereas those for $[Ni(L^1)_2]$ (**1**) and $[Ni(L^2)_2]$ (**2**) were grown by slow evaporation of their solutions in chloroform–methanol (1:1) mixture. Unit cell determination and intensity data collection for each crystal were carried out at room temperature (298 K) on a Bruker D8 Quest diffractometer fitted with a Photon 100 CMOS area detector and an Incoatec Microfocus Source for graphite monochromated Mo *Kα* radiation ($\lambda = 0.71073$ Å). Data acquisition, integration, and reduction were performed using the APEX3 software package.[11] The SADABS program[12] was employed for an empirical absorption correction. In the case of HL^1, some residual absorption effect was treated with an additional correction using the XABS2 program.[13] All four structures were solved by direct method and refined on F^2 using full-matrix least-squares procedures. The non-hydrogen atoms were refined anisotropically. The hydrogen atoms were included at idealized positions and refined as riding atoms with relative isotropic thermal parameters of their parent atoms. The SHELX-97 programs[14] available in the WinGX software suite[15] were used for structure solution and refinement. Mercury package[16] was used to prepare the structural illustrations. Selected crystallographic data for all four structures are listed in Table 1.

2.5 | General procedure for the Kumada–Corriu cross-coupling reaction

A mixture of aryl bromide (1.0 mmol), phenylmagnesium bromide (1.2 mmol), and the nickel complex catalyst (**1** or **2**) (0.05 or 0.1 mol%) in tetrahydrofuran (2 ml) was stirred at room temperature (25°C) under nitrogen

TABLE 1 Selected crystallographic data for HL^1, HL^2, $[Ni(L^1)_2]$ (**1**), and $[Ni(L^2)_2]$ (**2**)

Compound	HL^1	HL^2	1	2
Chemical formula	$C_{27}H_{30}N_2OS$	$C_{27}H_{29}N_2OClS$	$C_{54}H_{58}N_4O_2S_2Ni$	$C_{54}H_{56}N_4O_2Cl_2S_2Ni$
Formula weight	430.59	465.03	917.87	986.76
Crystal system	Triclinic	Triclinic	Triclinic	Triclinic
Space group	$P\bar{1}$	$P\bar{1}$	$P\bar{1}$	$P\bar{1}$
a (Å)	9.591(2)	10.8061(4)	9.2963(10)	8.4743(6)
b (Å)	10.479(2)	11.2035(5)	10.5788(11)	12.5662(9)
c (Å)	13.109(3)	12.1252(5)	13.5217(14)	12.8658(9)
α (°)	72.223(7)	73.437(2)	68.971(3)	97.861(2)
β (°)	86.174(9)	71.818(1)	80.553(4)	106.032(2)
γ (°)	85.211(7)	71.212(2)	80.439(4)	97.242(2)
V (Å^3)	1249.1(5)	1292.25(9)	1216.0(2)	1284.96(16)
Z	2	2	1	1
ρ (g cm^{-3})	1.145	1.195	1.253	1.275
μ (mm^{-1})	0.149	0.249	0.529	0.606
Reflections collected	17,449	31,846	34,745	45,530
Reflections unique	4228	4526	4259	4463
Reflections $I \geq 2\sigma(I)$	2289	3848	3451	4215
Parameters	280	293	290	299
$R1$, $wR2$ ($I \geq 2\sigma(I)$)	0.0909, 0.1645	0.0470, 0.1182	0.0549, 0.1465	0.0342, 0.0911
$R1$, $wR2$ (all data)	0.1962, 0.2038	0.0557, 0.1243	0.0702, 0.1599	0.0364, 0.0929
GOF on F^2	1.048	1.052	1.078	1.049
$\Delta\rho_{max}$, $\Delta\rho_{min}$ (e Å^{-3})	0.403, −0.308	0.432, −0.440	0.915, −0.860	0.401, −0.397

atmosphere for the required time. After that, the solvent was removed under reduced pressure, and the residue was purified by column chromatography on silica gel using *n*-hexane as the eluent to isolate the cross-coupled product.

3 | RESULTS AND DISCUSSION

3.1 | Synthesis and some properties

Reactions of equimolar amounts of benzyl bromide and *N*-(4-R-benzoyl)-*N*′-(2,6-diisopropylphenyl)thiourea (R = H and Cl) in presence of excess (1.7 times) NaH in tetrahydrofuran provided HL^1 and HL^2 in high yields (~85%) (Scheme 1). The complexes **1** and **2** were synthesized in good yields (~70%) by reacting one mole equivalent of $Ni(OAc)_2{\cdot}4H_2O$ with two mole equivalents of HL^1 and HL^2, respectively, in MeOH–$CHCl_3$ (1:1) mixture. The elemental analysis data of all four compounds are in good agreement with the corresponding molecular formulas. Magnetic susceptibility measurements with powdered samples of both complexes revealed their diamagnetic character. The complexes are insoluble in most of the common organic solvents such as methanol, ethanol, acetonitrile, dimethylsulfoxide, and *N*,*N*-dimethylformamide. However, they readily dissolve in dichloromethane and chloroform and provide brown solutions. In solution, they are electrically nonconducting. The use of bivalent nickel starting material for synthesis and the diamagnetic and nonelectrolytic character indicate that both **1** and **2** are square-planar nickel(II) complexes.

3.2 | X-ray structures

All of HL^1, HL^2, **1**, and **2** crystallize in the triclinic $P\bar{1}$ space group. The asymmetric units of HL^1 and HL^2 contain one complete molecule of the corresponding compounds. On the other hand, each of the two complex molecules is centrosymmetric, and the metal center resides at the inversion center. Thus, the asymmetric units of both **1** and **2** have half of the corresponding complex molecules. The molecular structures of HL^1 and HL^2 are illustrated in Figure 1, whereas those of **1** and **2** are

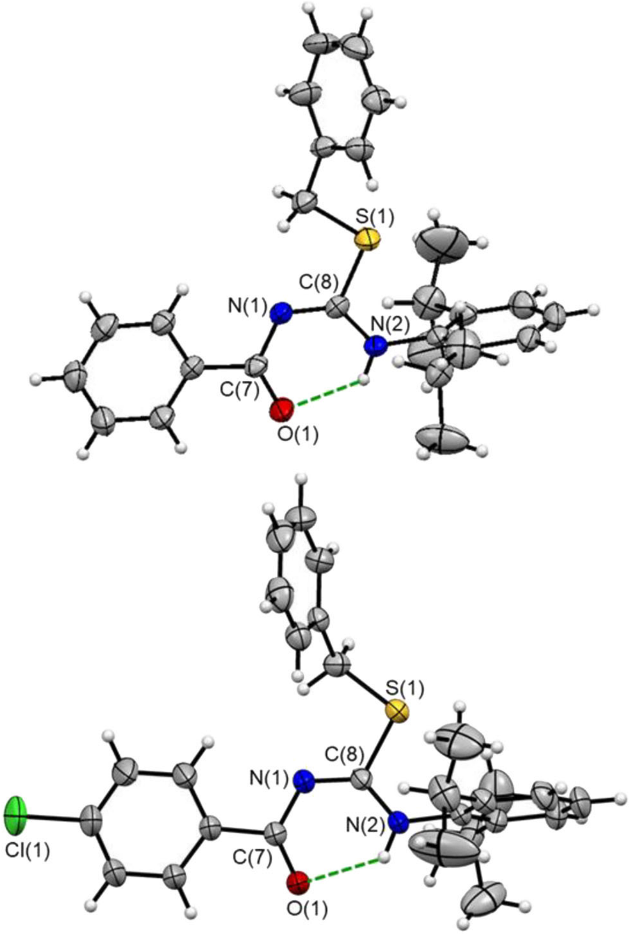

FIGURE 1 Molecular structures of HL^1 (top) and HL^2 (bottom). All nonhydrogen atoms are represented by their thermal ellipsoids at the 40% probability level. Only selected atoms are labeled for clarity

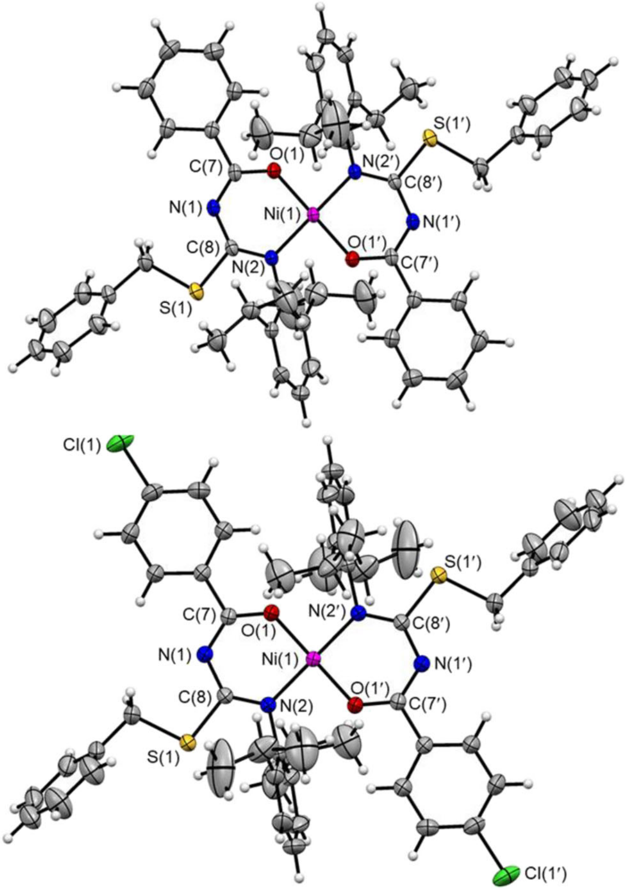

FIGURE 2 Perspective views of $[Ni(L^1)_2]$ (**1**) (top) and $[Ni(L^2)_2]$ (**2**) (bottom). The thermal displacement ellipsoids of the nonhydrogen atoms are drawn at the 40% probability level. Only selected atoms are labeled for clarity

shown in Figure 2. Selected bond parameters are listed in Tables 2 and 3.

Both HL^1 and HL^2 can have two forms amide and imino-ketone (Scheme 1) due to amine-imine tautomerism.[17] The X-ray structures revealed that both molecules exist in the imino-ketone form (Figure 1). The shorter C(8)—N(1) bond length compared with the C(8)—N(2) bond length indicates the double bond character of the former (Table 2). The C(7)—O(1) and C(7)—N(1) bond lengths are consistent with double and single bond characters, respectively. There is an intramolecular N—H···O hydrogen bond involving the amine and the keto-O leading to the formation of a planar six-membered ring (rms deviations: 0.02 and 0.08 Å for HL^1 and HL^2, respectively) in each structure. The N···O distance and the N—H···O angle are 2.638(3) Å and 128° for HL^1 and 2.677(2) Å and 126° for HL^2. It appears that the imino-ketone form is favored over the amide form due to this N—H···O interaction. The remaining intramolecular bond lengths and angles are unexceptional in both structures.

The structures of **1** and **2** confirm the deprotonation of the migratory proton and the monoanionic state of the ligands $(L^1)^-$ and $(L^2)^-$ (Figure 2). In the complexes, the C(7)—O(1) bond length is ~0.04 Å longer and C(7)—N(1) bond length is ~0.06 Å shorter compared with the corresponding bond lengths in HL^1 and HL^2 (Table 2). Hence, the imino-ketone fragment of the ligand is in the iminolate state in both **1** and **2**.[18,19] In contrast to HL^1 and HL^2, the C(8)—N(1) is longer and C(8)—N(2) is shorter in **1** and **2** (Table 2) indicating the single and double bond characters, respectively. In each centrosymmetric complex, the ligand coordinates the metal center through the iminolate-O and the azomethine-N atoms and forms a six-membered chelate ring with bite angle close to 90° (Table 3). Because of the inversion center at the coordinated metal atom, two ligands form a near perfect square-planar *trans*-NiN_2O_2 coordination geometry (Figure 2). The Ni—N and Ni—O bonds lengths are very similar in **1** and **2**, and they are within the ranges

TABLE 2 Selected bond lengths (Å) and angles (°) for HL^1, HL^2, **1**, and **2**

Compound	HL^1	HL^2	$[Ni(L^1)_2]$ (1)	$[Ni(L^2)_2]$ (2)
C(7)—O(1)	1.239(4)	1.229(2)	1.278(3)	1.272(2)
C(7)—N(1)	1.373(4)	1.364(2)	1.308(3)	1.309(2)
C(8)—N(1)	1.314(4)	1.312(2)	1.341(3)	1.343(2)
C(8)—N(2)	1.326(4)	1.327(2)	1.320(4)	1.314(2)
C(8)—S(1)	1.766(3)	1.768(2)	1.774(3)	1.771(2)

TABLE 3 Metal centered bond lengths (Å) and angles (°) for **1** and **2**

Complex	1	2
Ni(1)—O(1)	1.8215(19)	1.8342(12)
Ni(1)—N(2)	1.911(2)	1.9000(13)
Ni(1)—O(1′)[a]	1.8215(19)	1.8342(12)
Ni(1)—N(2′)[a]	1.911(2)	1.9000(13)
O(1)—Ni(1)—N(2)	91.58(9)	91.64(5)
O(1)—Ni(1)—O(1′)[a]	180.000(1)	180.00(7)
O(1)—Ni(1)—N(2′)[a]	88.42(9)	88.36(5)
N(2)—Ni(1)—O(1′)[a]	88.42(9)	88.36(5)
N(2)—Ni(1)—N(2′)[a]	180.0	180.00(9)
O(1′)[a]—Ni(1)—N(2′)[a]	91.58(9)	91.64(5)

[a] Symmetry transformations used to generate equivalent atoms: $-x$, $-y$, $-z + 2$ for **1** and $-x$, $-y$, $-z$ for **2**.

observed for nickel(II) square-planar complexes with ligands having comparable coordinating atoms.[19,20]

A possible explanation for the observed O,N-coordination mode instead of the O,S-coordination mode of $(L^{1/2})^-$ in **1** and **2** despite relatively more steric crowding around N-atom compared with that around S-atom is as follows. The delocalization of the negative charge by resonance is possible only in the O,N-coordination mode, but not in the O,S-coordination mode (Scheme 1). Further the C—O and C—N bond lengths in the six-membered chelate rings of the two complexes are in the range 1.272(2)–1.343(2) Å. However, the average C(8)—S(1) bond is ~0.46 Å longer than these bonds in $HL^{1/2}$ as well as in the corresponding complexes **1** and **2** (Table 2). Hence, it is very likely that the effective delocalization of the negative charge of the ligand with the formation of a relatively more uniform six-membered chelate ring leads to the O,N-coordination mode over the O,S-coordination mode of $(L^{1/2})^-$ in the present complexes. In the previously reported square-planar nickel(II) complexes with *N*,*N*-dialkyl/diaryl-*N*′-(aroyl) thioureates,[7] which are somewhat analogous to the present ligands, the opposite O,S-coordination was preferred over the O,N-coordination. In these complexes, resonance delocalization of the negative charge of the ligand is possible only in the O,S-coordination mode but not in the O,N-coordination mode. Thus, it appears that the coordination mode of the reported thioureates as well as the present deprotonated thiopseudoureas is dictated by the delocalization of the ligand negative charge and not by the steric crowding around the coordinating atom.

3.3 | Spectroscopic properties

Infrared spectra of HL^1, HL^2, **1**, and **2** were recorded in the range 4000–500 cm^{-1} using the ATR mode (Figures S1 and S2). The spectra display several bands of various intensities. No attempt was made to assign all the bands except for the following few. Both HL^1 and HL^2 show a somewhat broad band at ~3180 cm^{-1} due to the N—H stretching. Two medium intensity bands at ~1670 and 1598 cm^{-1} are assigned to the C═O and C═N stretches, respectively.[18,19] In contrast, neither of **1** and **2** displays the N—H and C═O stretching bands. Absence of these bands indicates the deprotonation of HL^1 and HL^2 and formation of the iminolate states $(L^1)^-$ and $(L^2)^-$ in the complexes. A medium intensity band observed at ~1584 cm^{-1} for both complexes is attributed to the metal coordinated C═N stretching.[18,19]

The electronic absorption spectra of **1** and **2** were recorded using their chloroform solutions. The spectral profiles of the two complexes are very similar (Figure 3). In each spectrum, two low intensity absorptions, a shoulder at 600 nm and a peak at 502 nm, are followed by three strong shoulders at ~400, ~355, and 330 nm and two very strong peaks at 303 and ~250 nm. Square-planar nickel(II) complexes are reported to exhibit weak spin-allowed ligand field transitions in the range 645–460 nm.[19a,b,20] Thus, the first two weak absorptions are assigned to ligand field transitions. Considering that each of HL^1 and HL^2 in chloroform displays an absorption

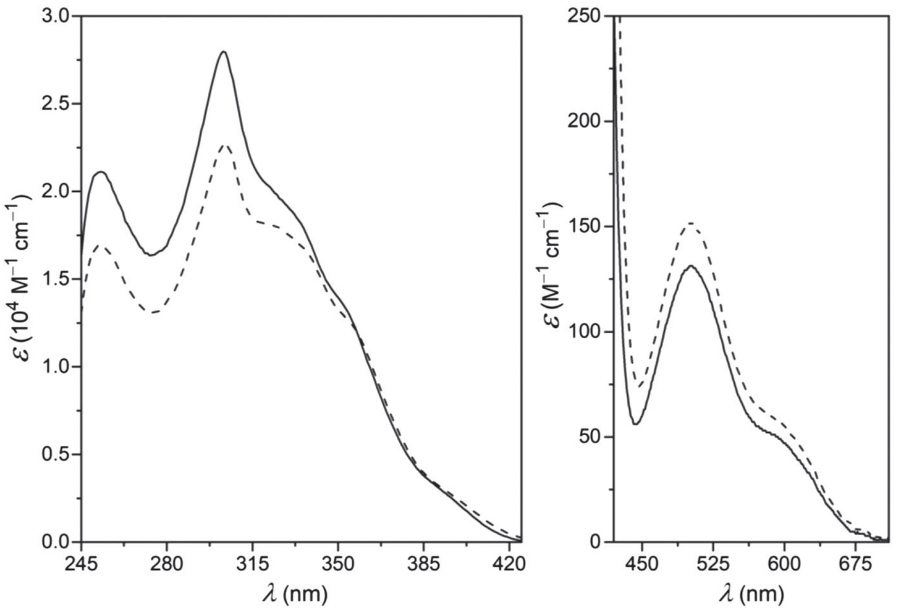

FIGURE 3 Electronic spectra of $[Ni(L^1)_2]$ (**1**) (—) and $[Ni(L^2)_2]$ (**2**) (------) in chloroform

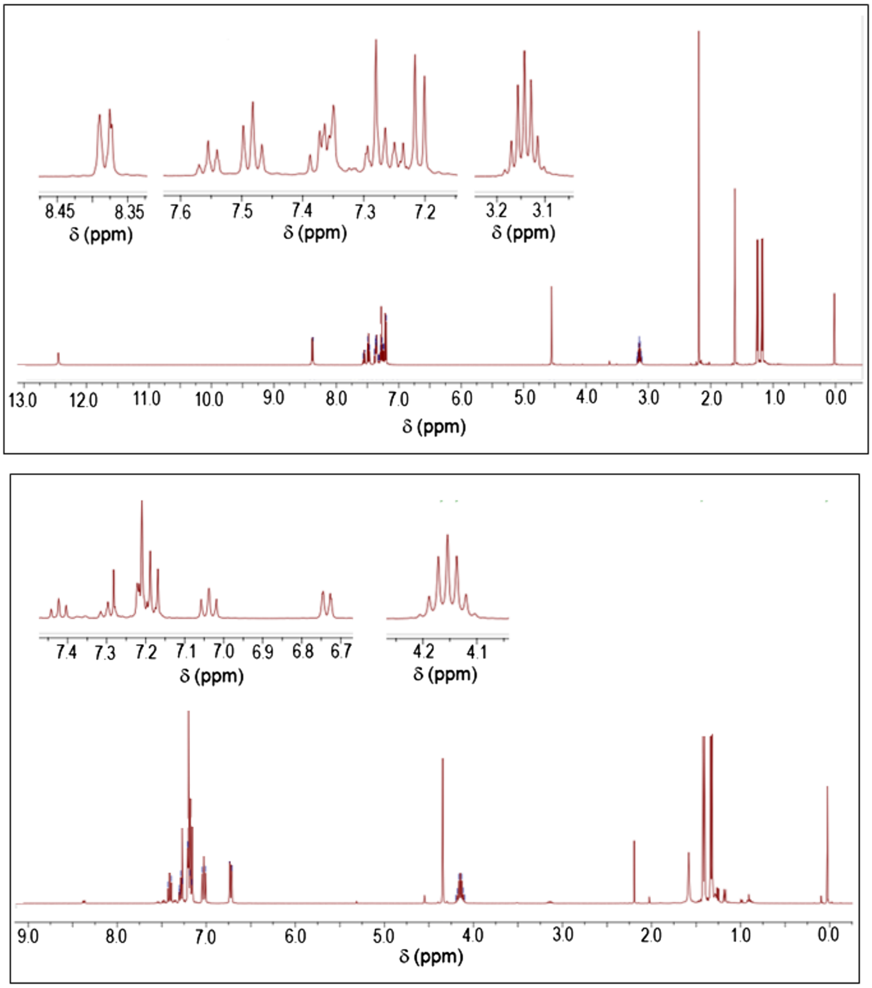

FIGURE 4 ^1H NMR spectra of HL^1 (top) and $[Ni(L^1)_2]$ (**1**) (bottom) in $CDCl_3$

maximum at ~295 nm followed by a shoulder at ~260 nm both being very strong, three strong shoulders observed for the complexes are attributed to ligand-to-metal charge transfer transitions[19,20] and the last two very strong highest energy peaks are assigned to intra-ligand transitions.

The proton NMR spectra of HL^1, HL^2, **1**, and **2** were recorded in $CDCl_3$. The chemical shift data (numbering scheme in Scheme 1) are given in Section 2 under the respective compounds, and the spectra of HL^1 and **1** are depicted in Figure 4, whereas the spectra of HL^2 and **2** are shown in Figure S3. The spectrum of each of the two complexes **1** and **2** clearly indicates that in solution also the two ligands are equivalent as observed in the corresponding X-ray structure. Both thiopseudoureas HL^1 and HL^2 display a singlet at ~12.43 ppm due to the NH group. As expected, neither of **1** and **2** shows this signal due to the deprotonation of the NH group and the monoanionic state of the ligand. The tertiary H-atoms of the two isopropyl groups of HL^1 and HL^2 appear as a two-proton septate at ~3.14 ppm, whereas the two-proton septate for the same H-atoms is shifted downfield by ~1 ppm in the cases of **1** and **2**. Unlike the single signal for the tertiary H-atoms, the methyl protons of the two isopropyl groups resonate as two closely spaced six-proton doublets for all four compounds. These two doublets are observed at ~1.25 and 1.18 ppm for the thiopseudoureas (HL^1 and HL^2), while they move slightly downfield to ~1.41 and 1.33 ppm for the complexes (**1** and **2**). The methylene protons of the benzyl group appear as a two-proton singlet at ~4.54 ppm for HL^1 and HL^2. However, in contrast to the protons of the isopropyl groups, the two-proton singlet due to the benzylic methylene protons in the complexes (**1** and **2**) appears slightly upfield at ~4.33 ppm. The aromatic protons of HL^1 and HL^2 resonate in the range 7.21–8.38 ppm whereas those for **1** and **2** are observed in relatively upfield and somewhat narrow range of 6.61–7.42 ppm with the expected splitting patterns.

3.4 | Catalytic studies

Optimization of the reaction conditions for C—C cross-coupling was performed using 1-bromo-4-methoxybenzene (1.0 mmol) and phenylmagnesium bromide (1.2 mmol) as the model substrates and the complexes **1** and **2** as catalysts in 2 ml of solvent (toluene and or tetrahydrofuran) (Table 4). All the reactions were carried out at room temperature (25°C). Using toluene as solvent and 0.05 mol% of **1** under nitrogen atmosphere, 80% yield was obtained in 24 h (Entry 1). In the mixed solvent toluene–tetrahydrofuran (1:1), the yield decreased considerably (Entry 2). In contrast, better yield (88%) was obtained in much less time in pure tetrahydrofuran (Entry 3). However, if the reaction was conducted in air keeping all other conditions the same as in Entry 3, the yield decreased drastically (Entry 4). Doubling of the catalyst loading increased the yield but by a very small amount (4%). Both **1** and **2** showed good and comparable catalytic activities and provided the coupling product in essentially the same yield (88 and 90%) under the same conditions (Entries 3 and 6). The homo-coupling product biphenyl was also produced but in very little amount (~4%). Therefore, the conditions used for Entry 3 were found to be optimal for reactions of phenylmagnesium bromide with aryl bromides using **1** or **2** as catalyst.

The substrate scope of the above coupling reaction was probed using **1** as the catalyst. The results are summarized in Table 5. Reactions of phenylmagnesium bromide with *para*-substituted bromobenzenes (4-F, 4-Cl, 4-Me, and 4-OMe) and 2-bromonaphthalene produced

TABLE 4 Optimization of reaction conditions

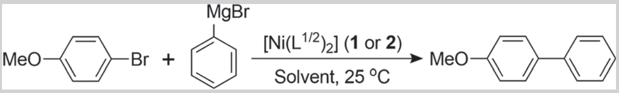

Entry	Catalyst	Catalyst loading (mol%)	Solvent	Time (h)	Yield[a] (%)
1	$[Ni(L^1)_2]$ (**1**)	0.05	Toluene	24[b]	80
2	$[Ni(L^1)_2]$ (**1**)	0.05	Toluene–THF (1:1)	24[b]	68
3	$[Ni(L^1)_2]$ (**1**)	0.05	THF	6[b]	88
4	$[Ni(L^1)_2]$ (**1**)	0.05	THF	12[c]	40
5	$[Ni(L^1)_2]$ (**1**)	0.10	THF	6[b]	92
6	$[Ni(L^2)_2]$ (**2**)	0.05	THF	6[b]	90

Note: BrC_6H_4OMe: 1.0 mmol; phenylmagnesium bromide: 1.2 mmol; solvent: 2 ml.

[a] Isolated yield.

[b] In nitrogen.

[c] In air.

TABLE 5 Coupling reactions of phenylmagnesium bromide with various aryl bromides

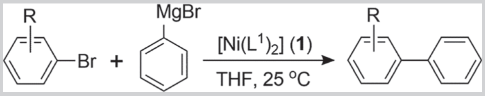

Entry	Aryl bromide	Product	Time (h)	Yield[a] (%)
1	1-Bromo-4-fluorobenzene	4-Fluorobiphenyl	6	96[b]
2	1-Bromo-4-chlorobenzene	4-Chlorobiphenyl	6	94[b]
3	1-Bromo-4-methylbenzene	4-Methylbiphenyl	6	93[b]
4	1-Bromo-4-methoxybenzene	4-Methoxybiphenyl	6	88[b]
5	2-Bromonaphthalene	2-Phenylnaphthalene	6	86[b]
6	1-Bromo-3-methylbenzene	3-Methylbiphenyl	12	92[b]
7	1-Bromo-3-methoxybenzene	3-Methoxybiphenyl	12	88[b]
8	1-Bromo-2-methylbenzene	2-Methylbiphenyl	24	86[c]
9	1-Bromo-2-methoxybenzene	2-Methoxybiphenyl	24	83[c]

Note: Aryl bromide: 1.0 mmol; phenylmagnesium bromide: 1.2 mmol; THF: 2 ml.
[a] Isolated yield.
[b] $[Ni(L^1)_2]$: 0.05 mol%.
[c] $[Ni(L^1)_2]$: 0.1 mol%.

the desired products in 86–96% yields in 6 h (Entries 1–5). The reactions of *meta*-substituted bromobenzenes (3-Me and 3-OMe) with phenylmagnesium bromide also provided high yields (92% and 88%) of the corresponding products (Entries 6 and 7) but in double reaction time (12 h) compared with that (6 h) required for the reactions of the *para*-substituted bromobenzenes with the same Grignard reagent. In contrast, the cross-coupling reactions of *ortho*-substituted bromobenzenes (2-Me and 2-OMe) with phenylmagnesium bromide require much longer reaction time (24 h) and double catalyst loading (0.1 mol%) compared with those needed for the coupling of *para*- and *meta*-substituted bromobenzenes with phenylmagnesium bromide to afford the products 2-methylbiphenyl and 2-methoxybiphenyl in slightly lower yields of 86% and 83%, respectively (Entries 8 and 9). The observed increase in the reaction time and the catalyst loading with the change of the substituent position on the bromobenzene from *para* to *meta* to *ortho* is in all likelihood to be due to the gradual increase of the steric hindrance. It may be noted that room temperature cross-coupling reactions for the synthesis of biaryls using nickel complexes as catalysts are not very common.[5,6] The present catalyst system not only works at room temperature but also provides as good as or improved yields when compared with the yields reported so far for nickel complex catalyzed reactions.

4 | CONCLUSIONS

In summary, two thiopseudoureas HL^1 and HL^2 and their corresponding nickel(II) complexes $[Ni(L^1)_2]$ and $[Ni(L^2)_2]$ have been successfully synthesized and characterized. The microanalytical data and diamagnetic and non-electrolytic characteristics of the two complexes indicate +2 oxidation state and square-planar coordination environment of the metal center in each complex. The X-ray structures of $HL^{1/2}$ showed the imino-ketone tautomeric form of both thiopseudoureas in the solid state, whereas the X-ray structures of $[Ni(L^{1/2})_2]$ confirmed the iminolate-O and azomethine-N donor coordination mode of the ligands $(L^{1/2})^-$ and a square-planar *trans*-N_2O_2 coordination geometry for both complexes. The spectroscopic features of all four compounds corroborate the corresponding molecular structures. Both complexes exhibit efficient catalytic activity toward Kumada–Corriu cross-coupling reactions of phenylmagnesium bromide with a variety of aryl bromides at room temperature. The reactions provided good to excellent yields of the biaryls.

ACKNOWLEDGMENTS

K.S. and A.K.S. thank the University Grants Commission (UGC), New Delhi, for research fellowships (Nos. 187/(CSIR-UGC NET June 2017) and F.25-1/2014-15 (BSR)/5-129/2007(BSR), respectively). G.N.B. thanks the Council of Scientific and Industrial Research (CSIR), New Delhi, for a research fellowship (No. 09/414(1025)/2012-EMR-I). S.K. thanks the UGC, New Delhi, for the Dr. D. S. Kothari postdoctoral fellowship (No. F.4-2/2006 (BSR)/13-1125/2013(BSR)). We thank the Ministry of Education, Government of India for financial assistance (Grant No. F11/9/2019-U3(A)) to the University of Hyderabad–Institute of Excellence. Financial and infrastructural supports from the UGC (through the CAS program, Grant No. F.540/2/CAS-111/2016(SAP-I)) and the Department of Science and Technology (DST), New Delhi (through the FIST program, Grant No. SR/FST/CST-030/2014(C)), are gratefully acknowledged.

AUTHOR CONTRIBUTIONS

Kinche Shakunthala: Investigation. **Ankit Kumar Srivastava:** Investigation. **G. Narendra Babu:** Investigation. **Srinivas Keesara:** Investigation. **Samudranil Pal:** Conceptualization; supervision.

DATA AVAILABILITY STATEMENT

CCDC 2049212–2049215 contain the supplementary crystallographic data for HL^1, HL^2, $[Ni(L^1)_2]$ (1), and $[Ni(L^2)_2]$ (2). These data can be obtained free of charge via http://www.ccdc.cam.ac.uk/conts/retrieving.html or from the Cambridge Crystallographic Data Centre, 12 Union Road, Cambridge CB2 1EZ, UK; fax: (+44) 1223-336-033; or e-mail: deposit@ccdc.cam.ac.uk. Additional data (Figures S1–S8) that support the findings of this study are available in the supplementary material of this article.

ORCID

Kinche Shakunthala https://orcid.org/0000-0002-1473-4940
Ankit Kumar Srivastava https://orcid.org/0000-0002-3195-5112
G. Narendra Babu https://orcid.org/0000-0001-6370-1371
Srinivas Keesara https://orcid.org/0000-0003-1991-2790
Samudranil Pal https://orcid.org/0000-0003-0217-8841

REFERENCES

[1] a) X. Chen, K. M. Engle, D.-H. Wang, J.-Q. Yu, *Angew. Chem., Int. Ed.* **2009**, *48*, 5094. b) R. Jana, T. P. Pathak, M. S. Sigman, *Chem. Rev.* **2011**, *111*, 1417. c) C. C. C. J. Seechurn, M. O. Kitching, T. J. Colacot, V. Snieckus, *Angew. Chem., Int. Ed.* **2012**, *51*, 5062. d) S. Xu, E. H. Kim, A. Wei, E. Negishi, *Sci. Technol. Adv. Mater.* **2014**, *15*, 044201. e) A. de Meijere, S. Bräse, M. Oestreich (Eds), *Metal Catalyzed Cross-Coupling Reactions and More*, Wiley-VCH **2014**. f) M. Busch, M. D. Wodrich, C. Corminboeuf, *ACS Catal.* **2017**, *7*, 5643. g) I. Kanwal, A. Mujahid, N. Rasool, K. Rizwan, A. Malik, G. Ahmad, S. A. A. Shah, U. Rashid, N. M. Nasir, *Catalysts* **2020**, *10*, 443. h) U. S. Kanchana, E. J. Diana, T. V. Mathew, G. Anilkumar, *Appl. Organomet. Chem.* **2020**, *34*, e5983.

[2] a) S. P. Stanforth, *Tetrahedron* **1998**, *54*, 263. b) J. Hassan, M. Sévignon, C. Gozzi, E. Schulz, M. Lemaire, *Chem. Rev.* **2002**, *102*, 1359. c) G. P. McGlacken, L. M. Bateman, *Chem. Soc. Rev.* **2009**, *38*, 2447. d) H. Aldemir, R. Richarz, T. A. M. Gulder, *Angew. Chem., Int. Ed.* **2014**, *53*, 8286. e) J. Wencel-Delord, A. Panossian, F. R. Leroux, F. Colobert, *Chem. Soc. Rev.* **2015**, *44*, 3418. f) S. Yuan, J. Chang, B. Yu, *Top. Curr. Chem.* **2020**, *378*, 23.

[3] K. Tamao, K. Sumitani, M. Kumada, *J. Am. Chem. Soc.* **1972**, *94*, 4374.

[4] R. J. P. Corriu, J. P. Masse, *J. Chem. Soc., Chem. Commun.* **1972**, 144.

[5] a) B. M. Rosen, K. W. Quasdorf, D. A. Wilson, N. Zhang, A.-M. Resmerita, N. K. Garg, V. Percec, *Chem. Rev.* **2011**, *111*, 1346. b) X. Hu, *Chem. Sci.* **2011**, *2*, 1867. c) M. M. Heravi, P. Hajiabbasi, *Monatsh. Chem.* **2012**, *143*, 1575. d) S. Z. Tasker, E. A. Standley, T. F. Jamison, *Nature* **2014**, *509*, 299. e) Z. Li, L. Liu, *Chin. J. Catal.* **2015**, *36*, 3. f) M. M. Heravi, V. Zadsirjan, P. Hajiabbasi, H. Hamidi, *Monatsh. Chem.* **2019**, *150*, 535. g) K. E. Poremba, S. E. Dibrell, S. E. Reisman, *ACS Catal.* **2020**, *10*, 8237.

[6] a) V. P. W. Böhm, T. Weskamp, C. W. K. Gstöttmayr, W. A. Herrmann, *Angew. Chem., Int. Ed.* **2000**, *39*, 1602. b) F.-L. Qing, R. Wang, B. Li, X. Zheng, W.-D. Meng, *J. Fluorine Chem.* **2003**, *120*, 21. c) Z.-X. Wang, L. Wang, *Chem. Commun.* **2007**, 2423. d) J. Berding, T. F. van Dijkman, M. Lutz, A. L. Spek, E. Bouwman, *Dalton Trans.* **2009**, 6948. e) N. Şahin, H. E. Moll, D. Sémeril, D. Matt, İ. Özdemir, C. Kaya, L. Toupet, *Polyhedron* **2011**, *30*, 2051. f) W. Dai, J. Xiao, G. Jin, J. Wu, S. Cao, *J. Org. Chem.* **2014**, *79*, 10537. g) V. Kuchtanin, L. Kleščíková, M. Šoral, R. Fischer, Z. Růžičková, E. Rakovský, J. Moncoľ, P. Segľa, *Polyhedron* **2016**, *117*, 90. h) L. Iffland, A. Petuker, M. van Gastel, U.-P. Apfel, *Inorganics* **2017**, *5*, 78. i) M. Mastalir, K. Kirchner, *Monatsh. Chem.* **2017**, *148*, 105. j) K. Matsubara, H. Yamamoto, S. Miyazaki, T. Inatomi, K. Nonaka, Y. Koga, Y. Yamada, L. F. Veiros, K. Kirchner, *Organometallics* **2017**, *36*, 255.

[7] a) R. del Campo, J. J. Criado, E. Garcia, M. R. Hermosa, A. Jiménez-Sánchez, J. L. Manzano, E. Monte, E. Rodríguez-Fernández, F. Sanz, *J. Inorg. Biochem.* **2002**, *89*, 74. b) G. Binzet, G. Kavak, N. Külcü, S. Özbey, U. Flörke, H. Arslan, *J. Chem.* **2013**, 536562. and references therein

[8] a) T. Iwamoto, T. Watano, M. Shigekawa, *J. Biol. Chem.* **1996**, *271*, 22391. b) T. P. Prakash, A. Püschl, M. Manoharan, *Nucleos. Nucleot. Nucl. Acids* **2007**, *26*, 149. c) M. Ferreira, L. S. Assunção, A. H. Silva, F. B. Filippin-Monteiro, T. B. Creczynski-Pasa, M. M. Sá, *Eur. J. Med. Chem.* **2017**, *129*, 151. d) J. Merad, J.-M. Pons, O. Chuzel, C. Bressy, *Eur. J. Org. Chem.* **2016**, 5589.

[9] a) K. Srinivas, P. Srinivas, P. S. Prathima, K. Balaswamy, B. Sridhar, M. M. Rao, *Catal. Sci. Technol.* **2012**, *2*, 1180. b) S. Thogiti, S. P. Parvathaneni, S. Keesara, *J. Organomet. Chem.* **2016**, *822*, 165.

[10] D. D. Perrin, W. L. F. Armarego, D. P. Perrin, *Purification of Laboratory Chemicals*, 2nd ed., Pergamon **1983**.

[11] APEX3, Program for Data Collection on Area Detectors, Bruker AXS Inc., Madison, Wisconsin, USA, **2016**.

[12] G. M. Sheldrick, SADABS, program for area detector absorption correction, University of Göttingen, Göttingen, Germany, **1997**.

[13] S. Parkin, B. Moezzi, H. Hope, *J. Appl. Crystallogr.* **1995**, *28*, 53.

[14] G. M. Sheldrick, *Acta Crystallogr. Sect. A* **2008**, *64*, 112.

[15] L. J. Farrugia, *J. Appl. Crystallogr.* **2012**, *45*, 849.

[16] F. Macrae, I. J. Bruno, J. A. Chisholm, P. R. Edgington, P. M. Cabe, E. Pidcock, L. Rodriguez-Monge, R. Taylor, J. van de Streek, P. A. Wood, *J. Appl. Crystallogr.* **2008**, *41*, 466.

[17] N. Phukan, J. B. Baruah, *Cryst. Eng. Comm.* **2016**, *18*, 3877.

[18] a) S. Das, S. Pal, *J. Organomet. Chem.* **2004**, *689*, 352. b) S. Das, S. Pal, *J. Organomet. Chem.* **2006**, *691*, 2575. c) A. R. B. Rao, S. Pal, *J. Organomet. Chem.* **2013**, *731*, 67.

[19] a) A. Mukhopadhyay, G. Padmaja, S. N. Pal, S. Pal, *Inorg. Chem. Commun.* **2003**, *6*, 381. b) A. Mukhopadhyay, S. Pal, *Polyhedron* **2004**, *23*, 1997. c) A. Mukhopadhyay, S. Pal, *Eur. J. Inorg. Chem.* **2006**, 4879. d) A. Mukhopadhyay, S. Pal, *Eur. J. Inorg. Chem.* **2009**, 4141. e) T. Ghosh, A. Mukhopadhyay, K. S. C. Dargaiah, S. Pal, *Struct. Chem.* **2010**, *21*, 147. f) G. N. Babu, S. Pal, *J. Chem. Sci.* **2017**, *129*, 1105.

[20] a) A. la Cour, M. Findeisen, R. Hazell, L. Hennig, C. E. Olsen, O. Simonsen, *J. Chem. Soc., Dalton Trans.* **1996**, 3437. b) C. Lochenie, S. Schlamp, A. P. Railliet, K. Robeyns, B. Weber, Y. Garcia, *Cryst. Eng. Comm.* **2014**, *16*, 6213.

SUPPORTING INFORMATION

Additional supporting information may be found online in the Supporting Information section at the end of this article.

How to cite this article: Shakunthala K, Srivastava AK, Babu GN, Keesara S, Pal S. Nickel (II) complexes with N,O-donor thiopseudourea ligands: Syntheses, structures, and catalytic applications in Kumada–Corriu cross-coupling reactions. *Appl Organomet Chem*. 2021;e6261. https://doi.org/10.1002/aoc.6261